

This article was downloaded by:

On: 22 January 2011

Access details: *Access Details: Free Access*

Publisher *Taylor & Francis*

Informa Ltd Registered in England and Wales Registered Number: 1072954 Registered office: Mortimer House, 37-41 Mortimer Street, London W1T 3JH, UK



## **The Journal of Adhesion**

Publication details, including instructions for authors and subscription information:

<http://www.informaworld.com/smpp/title~content=t713453635>

### **An In-Situ Failure Model for Adhesive Joints**

Shaw Ming Lee<sup>a</sup>

<sup>a</sup> Composite Materials Department, Ciba-Geigy Corporation, Fountain Valley, California, U.S.A.

**To cite this Article** Lee, Shaw Ming(1985) 'An In-Situ Failure Model for Adhesive Joints', *The Journal of Adhesion*, 18: 1, 1 – 15

**To link to this Article:** DOI: 10.1080/00218468508074933

**URL:** <http://dx.doi.org/10.1080/00218468508074933>

PLEASE SCROLL DOWN FOR ARTICLE

Full terms and conditions of use: <http://www.informaworld.com/terms-and-conditions-of-access.pdf>

This article may be used for research, teaching and private study purposes. Any substantial or systematic reproduction, re-distribution, re-selling, loan or sub-licensing, systematic supply or distribution in any form to anyone is expressly forbidden.

The publisher does not give any warranty express or implied or make any representation that the contents will be complete or accurate or up to date. The accuracy of any instructions, formulae and drug doses should be independently verified with primary sources. The publisher shall not be liable for any loss, actions, claims, proceedings, demand or costs or damages whatsoever or howsoever caused arising directly or indirectly in connection with or arising out of the use of this material.

# An In-Situ Failure Model for Adhesive Joints

SHAW MING LEE

*Ciba-Geigy Corporation, Composite Materials Department,  
Fountain Valley, California 92708, U.S.A.*

*(Received February 22, 1984; in final form May 16, 1984)*

In this paper, a theoretical model based on the fracture mechanics principle is built to describe the in-situ failure process of adhesive joints. The central concept of the model is that the adhesive fracture is controlled by the plastic zone developed at the crack tip. On the basis of an approximate crack tip stress distribution, a quantitative representation is found to relate the adhesive fracture energy  $G_{IC}(\text{joint})$  to certain bulk resin properties: fracture toughness  $G_{IC}(\text{bulk})$ , yield stress  $\sigma_y$ , and Young's modulus  $E$ . It is found that the factor  $\sigma_y^2/E$  is sometimes more important than  $G_{IC}(\text{bulk})$  in controlling  $G_{IC}(\text{joint})$ . The in-situ failure model interprets well the temperature and loading rate dependent phenomena of adhesive joint fracture reported in the literature. A correlation between the resin material variables and the adhesive fracture is thus established.

## INTRODUCTION

Adhesive bonds have been extensively used as an efficient means to join structural components with the advantage of good strength-to-weight ratio. The adhesive materials most often used are thermosetting polymers, such as epoxies. Although they usually provide adequate adhesion between the adhesive and the adherend, their relatively brittle mechanical properties present them as a potential weak link in the structure. This necessitates the study of the fracture behavior of adhesive joints. From the structural point of view, the adhesive fracture characteristics have to be established in order to design the adhesive joints efficiently. From the materials development standpoint, it is desirable

to understand the failure mechanisms involved in the adhesive joints. The important adhesive properties controlling failure can then be identified and optimized.

The fracture of adhesive joints has been studied with considerable success by using the fracture mechanics approach. In particular, adhesive joints with Mode I crack growth (tensile loading perpendicular to the crack plane) have been well characterized. Although the exact details of crack-tip deformation have yet to be solved, recent work<sup>1-5</sup> has led to a qualitative understanding about the failure behavior of adhesive bonds. It has become clear that the plastic zone developed at the crack tip determines the crack resistance of the bonds. The adhesive joint fracture energy  $G_{IC}(\text{joint})$ , defined by the strain energy release rate, can be attributed to the size of this zone. The work of Wang, *et al.*,<sup>6</sup> provides an especially important insight into the adhesive bond failure process. Their finite element calculations revealed the unique crack tip stress pattern in the adhesive bond of a double cantilever beam specimen. Based on Wang's results, Kinloch and Shaw<sup>4</sup> were able to give a quite reasonable argument about the observed dependence of  $G_{IC}(\text{joint})$  on bond thickness  $h$ .

It, therefore, appears that the plastic zone concept can indeed help to interpret the adhesive joint failure process. However, such a description of the failure behavior has been so far still qualitative due to the lack of detailed analysis of the crack tip stress field. The important adhesive material properties controlling the fracture process have remained unclear.

In this paper, a theoretical model is proposed to describe the *in-situ* failure process of adhesive joints. Based on the crack tip plastic zone concept, the model attempts to determine the plastic zone size as a function of the crack tip stress state. For this purpose, an approximate but reasonable crack tip stress distribution is proposed by considering the numerical results of Wang, *et al.*<sup>6</sup> A quantitative representation is then found to relate the adhesive fracture energy  $G_{IC}(\text{joint})$  to certain adhesive material properties. Interestingly, the fracture energy  $G_{IC}(\text{bulk})$  of the bulk adhesive material is only one of several variables controlling the failure process. The *in-situ* failure model introduced here has been successfully employed before to composite materials<sup>7</sup> to describe the failure process of transverse cracking which is quite similar to the adhesive fracture discussed here. When applied to adhesive joint failure, the model interprets well the phenomena of adhesive fracture reported in the literature. As a result,

the important adhesive material properties controlling adhesive joint failure are identified.

## IN-SITU FAILURE MODEL

### Approximate crack tip stress distribution

In our *in-situ* failure model proposed here, a plane crack at the center of the adhesive (Figure 1) is investigated for Mode I crack propagation characteristics. First, the stress pattern at the crack tip is approximated here in a parametric form based on the results from Wang *et al.*<sup>6</sup> Although the results were for a double cantilever beam specimen, the essential character of the stress distributions obtained should carry over to other adhesive joint specimens.

An important finding from Wang's study is that the stress pattern at the adhesive crack tip is quite different from that in a monolithic system. For a crack in an adhesive joint, the conventional  $r^{-1/2}$  singularity, where  $r$  is the distance from the crack tip, of stress distribution is confined in an extremely limited region. This region, much

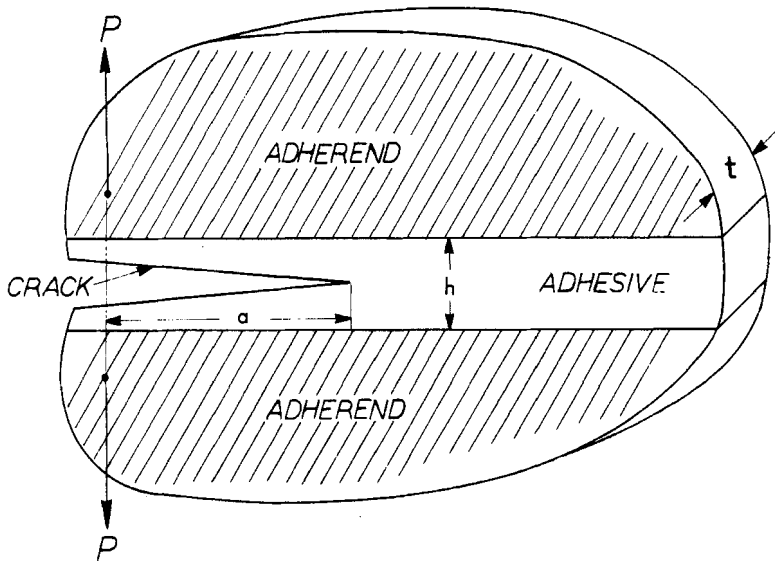


FIGURE 1 A crack in an adhesive joint subject to an applied load  $P$ .

smaller than that for a crack in a bulk material, was shown to be only a small fraction of the adhesive thickness. To illustrate this point, a typical log-log plot of  $\sigma_{22}/P$  versus  $x$ , the distance from the crack tip along axis 1, is shown in Figure 2 with  $P$  being the external load applied to the adhesive joint specimen. The curve is only linear with a slope of  $-1/2$ , meaning  $r^{-1/2}$  dependence, at small  $x$ . Further away from the tip, the stress gradient is much lower than that in the  $r^{-1/2}$  region. The slowly varying stress state extends from a distance of less than one adhesive thickness to several adhesive layer thickness ahead of the crack tip.

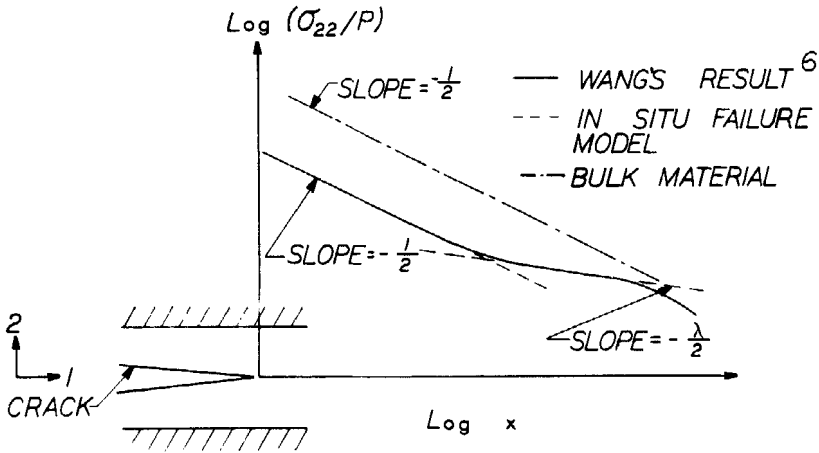


FIGURE 2 Adhesive crack tip  $\sigma_{22}$  distribution from Wang *et al.*<sup>6</sup> and the bi-linear approximation in this study.

Certain useful information can be drawn from the unique crack tip stress pattern in Figure 2. First of all, an important assumption is made here to approximate the log-log curve in Figure 2 in a piecewise linear manner. The localized region at the crack tip is represented by a straight line with a slope of  $-1/2$ . The region away from the crack tip with gradual decreasing stress can be fitted and represented by a straight line with a slope of  $-\lambda/2$ , where  $\lambda \ll 1$  is expected. Although the numerical value of  $\lambda$  is not immediately obvious, the physical significance of  $\lambda$  indicated by  $\lambda \ll 1$  will become clear later. The far field stress outside these two regions is considered not important for the failure process and

is not treated here. Such a bi-linear representation, although only approximate, does serve a useful purpose of quantifying the stress state.

### Plastic zone length

As the crack tip plastic zone controls the fracture behavior of adhesive joints, the development of the zone must be closely related to the stress pattern ahead of the crack. Based on the foregoing argument, the stress at the crack tip can be expressed by region of  $r^{-1/2}$  dependence and region of  $r^{-3/2}$  dependence, as shown in Figure 3. With the stress profile so determined, the plastic zone length  $l_p$  developed at the crack tip can then be estimated by considering it to be the region where  $\sigma_{22}$  is higher than the resin yield stress  $\sigma_y$ . Since the  $r^{-1/2}$  dependent

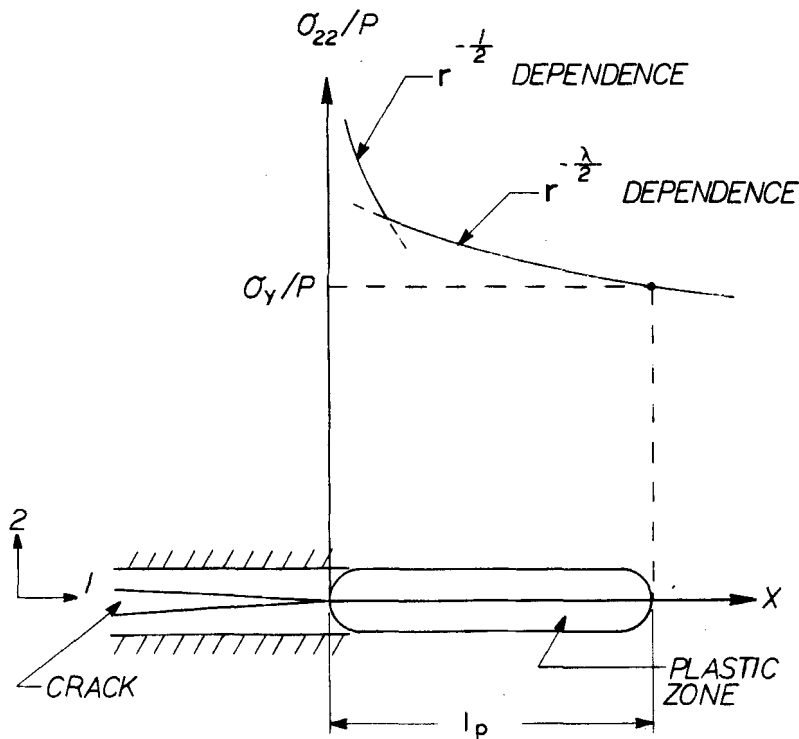


FIGURE 3 Schematic of the plastic zone developed at the crack tip in an adhesive joint.

stress is narrowly confined to the crack tip, it can be reasonably argued that  $l_p$  can extend to the region with stress of  $r^{-\lambda/2}$  dependence (shown in Figure 3). This is a major departure from the bulk resin fracture where the crack tip plastic zone is mainly determined by the  $r^{-1/2}$  dependent stress distribution.

### Adhesive fracture energy as a function of bulk adhesive properties

In a fracture toughness test, such as the double cantilever beam technique, the adhesive joint specimen with crack length  $a$  is under a gradually increasing load  $P$ . When the load reaches a critical value  $P_c$ , crack propagation takes place. The fracture energy of the adhesive joint  $G_{IC}(\text{joint})$  can be determined from the compliance calibration method as follows:

$$G_{IC}(\text{joint}) = (P_c^2/2t) (dC/da) \quad (1)$$

where  $C$  is the specimen compliance and  $t$  the specimen width (Figure 1).

The crack tip stress distribution induced by a given applied load  $P$  before crack propagation is dependent on the adhesive modulus  $E$ , and adherend modulus  $E'$ . From Wang *et al.*,<sup>6</sup> for fixed  $E'$  the stress intensity factor  $K_I$  to  $P$  ratio was found to be proportional to  $E^{1/2}$ . The level of  $\sigma_{22}/P$  profile in Figure 2 being directly proportional to  $K_I/P$  would, therefore, also be proportional to  $E^{1/2}$ .

As discussed before, the plastic zone can extend to the region with  $r^{-\lambda/2}$  dependent stress. For the purpose of generality, the stress region of interest is assumed to be  $r^{-m/2}$  dependent where  $m$  is a variable ranging from  $\lambda$  to 1, depending on where the plastic zone extends to. The stress  $\sigma_{22}$  in the  $r^{-m/2}$  dependent region can be expressed by:

$$(\sigma_{22}/P) \propto (E^{1/2} r^{-m/2}). \quad (2)$$

When the crack propagation takes place,  $G_{IC}(\text{joint})$  can be determined from Equation 1. From the above expression, the critical load  $P_c$  can be related to the plastic zone length  $l_p$  by:

$$P_c \propto (\sigma_y l_p^{m/2}/E^{1/2}). \quad (3)$$

The  $(dC/da)$  term in Equation 1, on the other hand, is almost in-

dependent of the plastic zone for the relatively brittle failure of our interest here.  $C$  and  $(dC/da)$  are, therefore, only related to the adherend properties. By using Equations 1, 3 and  $dC/da$  discussed above,  $G_{IC}(\text{joint})$  can be written as:

$$G_{IC}(\text{joint}) = l\sigma_y^2 l_p^m / E \quad (4)$$

where  $F$  is only a function of adherend modulus and bond thickness.

In order to relate  $G_{IC}(\text{joint})$  to the properties of the bulk adhesive, a failure criterion is needed to assess the critical value of  $l_p$  for crack propagation.  $l_p$  is assumed to be related to the critical plastic zone radius  $r_p$  in the bulk adhesive material.  $r_p$  is given by<sup>1-5,8</sup>:

$$r_p = EG_{IC}(\text{bulk}) / (6\pi (1-\nu^2) \sigma_y^2), \quad (5)$$

where  $G_{IC}(\text{bulk})$  and  $\nu$  are the fracture energy and Poisson's ratio, respectively, of the bulk adhesive. As a first order approximation, it is assumed that  $l_p$  is proportional to  $r_p$  for fixed bond thickness and adherend modulus, *i.e.*,

$$l_p = Sr_p \quad (6)$$

where  $S$  is a constant.  $G_{IC}(\text{joint})$  in Equation 4 can then be rewritten as:

$$G_{IC}(\text{joint}) = H\sigma_y^2 r_p^m / E \quad (7)$$

where  $H = FS^m$ .

By substituting Equation 5 into Equation 7,  $G_{IC}(\text{joint})$  can be found to be:

$$G_{IC}(\text{joint}) = M(\sigma_y^2/E)^{1-m} G_{IC}^m(\text{bulk}) \quad (8)$$

where  $M = H/(6\pi (1-\nu^2))^m$ .

Alternatively, by expressing  $\sigma_y^2/E$  in terms of  $G_{IC}(\text{bulk})$  and  $r_p$ , Equation 7 becomes:



$$G_{IC}(\text{joint}) = L(G_{IC}(\text{bulk})/r_p)^{1-m} G_{IC}^m(\text{bulk}) \quad (9)$$

where  $L = H/(6\pi(l - \nu^2))$ .

Equations 7, 8 and 9 are the basic equations correlating  $G_{IC}(\text{joint})$  with bulk adhesive material variables. The physical implication of Equation 7 is that a desired adhesive material to resist crack should not only have large enough plastic zone size but also high enough  $\sigma_y^2/E$  value in the zone. This is also reflected in Equation 9 that  $(G_{IC}(\text{bulk})/r_p)$  dictates how effectively  $G_{IC}(\text{bulk})$  translates into  $G_{IC}(\text{joint})$ . Equation 8, being expressed in terms of all measurable variables, will be focused on for all further discussion. It can be seen from this equation that  $\sigma_y^2/E$  is at least as important as  $G_{IC}(\text{bulk})$  in contributing to  $G_{IC}(\text{joint})$ .

It is revealing from the model that  $G_{IC}(\text{joint})$  is not solely determined by  $G_{IC}(\text{bulk})$ . Other variables,  $\sigma_y$  and  $E$ , are also important in contributing to the adhesive joint fracture. Physically, it means that the failure process of a material is critically dependent on the detailed crack tip stress distribution. Thus  $G_{IC}(\text{bulk})$  of an unconstrained bulk material may not necessarily translate directly into the fracture energies of the same material under different constrained conditions.

### Residual stress consideration

As observed in our study on composite materials,<sup>7</sup> the residual stress in the resin due to the thermal mismatch between resin and fibers during curing has a significant effect on the fracture behavior of composites. The residual stress would also exist in the adhesive joint as a result of the thermal mismatch between the adhesive and the adherends.

For the planar adhesive layer studied here, the residual stress is, however, expected to be plane stress in nature with components in the plane of the resin layer. The residual stress perpendicular to the plane of the resin layer should disappear as no constraint to the adhesive is present in that direction. As Mode I failure of adhesive joint discussed here is mainly controlled by the stress induced perpendicular to the plane of the resin layer, the residual stress is not expected to influence the induced  $\sigma_{22}$  stress profile such as that in Figure 2. The residual stress, however, can change  $\sigma_y$  in the 2-direction to some extent. As long as the residual stress is small compared with  $\sigma_y$ , assumed to be the case here,  $\sigma_y$  will not be changed appreciably. The contribution

from the residual stress to  $G_{IC}(\text{joint})$  is assumed to be negligible in our model.

## DISCUSSION

The *in-situ* failure model will be applied here to interpret some well-observed fracture behaviour of adhesive joints reported in the literature. The data to be discussed are mostly taken from experiments using, but not limited to, double cantilever beam type of specimens. The fracture energies  $G_{IC}(\text{joint})$  of adhesive joints are, in general, a function of a number of possible test parameters as well as specimen parameters. For example, the pioneering studies by Bascom *et al.*<sup>1,2</sup> found that  $G_{IC}(\text{joint})$  is dependent on bond thickness. In addition,  $G_{IC}(\text{joint})$  would be affected by temperature<sup>1-4,8,9</sup> and test rate<sup>3-5,11</sup>.

$G_{IC}(\text{joint})$  has been observed<sup>1-5</sup> to be a function of bond thickness  $h$  with a maximum value at  $h$  equal to  $2r_p$ . In our *in-situ* model introduced earlier, the bond thickness effect would, in principle, be a factor in deciding the plastic zone size  $l_p$  at crack propagation. However, in the absence of an exact crack tip failure criterion,  $l_p$  could only be qualitatively related to bulk adhesive critical plastic zone size (Equation 6). Other key parameters  $m$  and  $F$  (Equation 4) controlling  $G_{IC}(\text{joint})$  in relation to  $h$  can not be accurately deduced because of insufficient analysis of crack tip stress at different  $h$ . The joint thickness effect, therefore, can not be explicitly determined from our model at the moment.

The phenomena of temperature as well as test rate dependence of  $G_{IC}(\text{joint})$  at constant bond thickness, on the other hand, can be readily interpreted by our model. The relative importance of adhesive material variables implied by such phenomena can, therefore, be demonstrated here. The temperature and test rate effects will be addressed individually as follows:

### Temperature effect

In Ting and Cottingham's work<sup>9</sup>, the adhesive fracture energies  $G_{IC}(\text{joint})$  of two thermosetting resins (C-10 and SR 5208) as a function of temperature were reported. The surprising finding there was that the  $G_{IC}(\text{joint})$  decreases as the temperature is increased. This appears to be contrary to the fracture behavior of bulk resin where  $G_{IC}(\text{bulk})$  usually increases with increasing temperature. The observed

phenomenon can, however, be readily interpreted by our *in-situ* failure model.

From equation 8,  $G_{IC}(\text{joint})$  is a function of both  $G_{IC}(\text{bulk})$  and  $(\sigma_y^2/E)$ . Although  $G_{IC}(\text{bulk})$  increases with increasing temperature, both  $\sigma_y$  and  $E$  decrease with increasing temperature. In general, the rate of change of  $\sigma_y$  as a function of temperature is much higher than that of  $E^{10}$ . The factor  $(\sigma_y^2/E)$  would therefore decrease with increasing temperature.

As discussed before, the plastic zone can extend to the region of  $r^{-\lambda/2}$  dependence with  $\lambda \ll 1$ . In this case,  $G_{IC}(\text{joint})$  from Equation 8 with  $m = \lambda$  is expected to be a stronger function of  $(\sigma_y^2/E)$  than of  $G_{IC}(\text{bulk})$ .  $G_{IC}(\text{joint})$  will follow the trend of decreasing  $(\sigma_y^2/E)$  as the temperature is increased. This explains Ting and Cottingham's finding mentioned above.

In the paper by Bascom and Cottingham,<sup>2</sup> the fracture behavior of adhesive joints with an elastomer-epoxy resin system as the adhesive was studied. Bulk as well as fracture adhesive energies were determined using the tapered double cantilever beam specimens. In their study, not only the important thickness dependence but also the temperature effect on  $G_{IC}(\text{joint})$  were reported. Moreover, quite complete information of relevant bulk resin properties was collected. It is, therefore, of interest to apply our *in-situ* failure model here to correlate the bulk properties with adhesive joint fracture energies of this system.

The bulk material properties, fracture energy  $G_{IC}(\text{bulk})$ , modulus  $E$  and yield stress  $\sigma_y$ , at different temperature levels obtained from Bascom's paper<sup>2</sup> are given in Table I. Note that  $\sigma_y$  is estimated here, as was in the original paper, from the tensile test results on bulk materials. The values of  $\sigma_y$  are only approximate as pointed out by Gledhill and Kinloch<sup>8</sup> since none of the adhesives exhibit bulk yielding in uniaxial tension. However, as a first order approximation the true yield stress of the material is assumed to be proportional to  $\sigma_y$  determined here. This should not appreciably affect the applicability of our model as can be seen from Equation 8 where  $G_{IC}(\text{joint})$  is a power function of the true yield stress and thus  $\sigma_y$ . The fracture energy  $G_{IC}(\text{joint})$  of the adhesive joint at different temperatures are also given in Table I for bond thickness of 0.25 mm.

To facilitate the correlation, Equation 8 is rearranged and transformed into a logarithmic expression:

$$\log(G_{IC}(\text{joint})/G_{IC}(\text{bulk})) = \log M + (1-m)\log(\sigma_y^2/EG_{IC}(\text{bulk})). \quad (10)$$

IN-SITU FAILURE MODEL

TABLE I  
Experimental results from Bascom and Cottingham<sup>2</sup> and estimated  $G_{IC}(\text{joint})$  from the *in-situ* failure model

Temperature (°C)	Experimental results				<i>In-situ</i> failure model		
	$\sigma_y$ (Mpa)	$E$ (Gpa)	$G_{IC}(\text{bulk})$ (kJ/m <sup>2</sup> )	$G_{IC}(\text{joint})$ (kJ/m <sup>2</sup> )	$G_{IC}(\text{joint})$		$m = 0.53$ $M = 2.1$
					$m \approx 0$	$M = 3.5$	
50	32	1.67	7.75	2.0	1.9	—	—
37	38	1.94	5.25	2.1	2.3	—	—
25	47	2.17	3.13	3.5	3.3	—	—
0	55	2.39	1.63	2.8	—	—	3.0
-20	64	2.53	1.25	3.2	—	—	2.9
-40	71	2.72	0.75	2.3	—	—	2.4

The original power function in Equation 8 is, thus, reduced to a linear function in the above equation.

For this particular system,  $G_{IC}(\text{joint})$  only follows the trend of  $(\sigma_y^2/E)$  at temperature above  $0^\circ\text{C}$ . Below  $0^\circ\text{C}$ ,  $G_{IC}(\text{joint})$  appears to follow the trend of  $G_{IC}(\text{bulk})$  which decreases with decreasing temperature. This suggests that  $m = \lambda \ll 1$  discussed before only applies to temperature above  $0^\circ\text{C}$ . Below  $0^\circ\text{C}$ ,  $m$  may not be much smaller than one. The possible explanation is that the plastic zone growth is gradually limited by the increasing  $\sigma_y$  as temperature decreases. For this resin system with the given bond thickness, the front of plastic zone below  $0^\circ\text{C}$  may be constrained to a region where the  $r^{-\lambda/2}$  dependent stress in our bi-linear approximation is no longer accurate (see Figure 4). As shown in Figure 4, however, the log-log stress profile of interest can be approximated by a multiple linear curve. The plastic zone front can be considered to be in an  $r^{-\lambda'/2}$  stress region with  $\lambda'$  larger than  $\lambda$  in the bi-linear case. In this case,  $m$  in Equation 8 or 10 would be equal to  $\lambda'$ .

In view of the dependence of  $m$  on temperature for this system, correlations are carried out separately for two sets of data: the low temperature set ( $-40^\circ\text{C}$ ,  $-20^\circ\text{C}$  and  $0^\circ\text{C}$ ) and the high temperature set ( $20^\circ\text{C}$ ,  $37^\circ\text{C}$  and  $50^\circ\text{C}$ ). Each set is assumed to have its own  $M$  and  $m$  values.

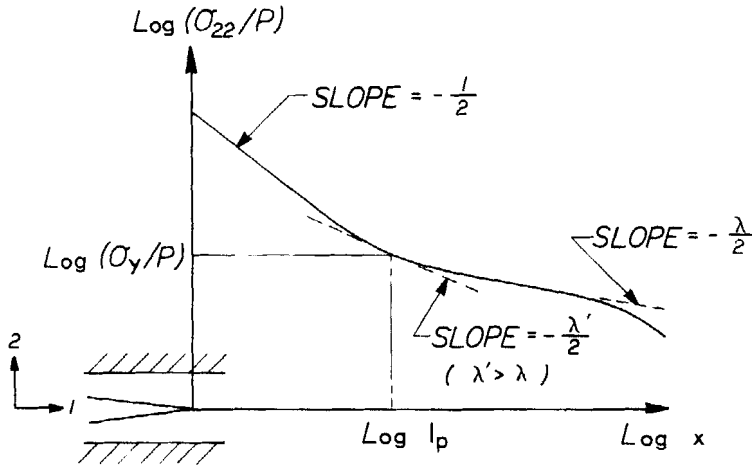


FIGURE 4 Schematic of the front of plastic zone extended to a region with stress of  $r^{-\lambda'/2}$  dependence where  $\lambda' > \lambda$ .

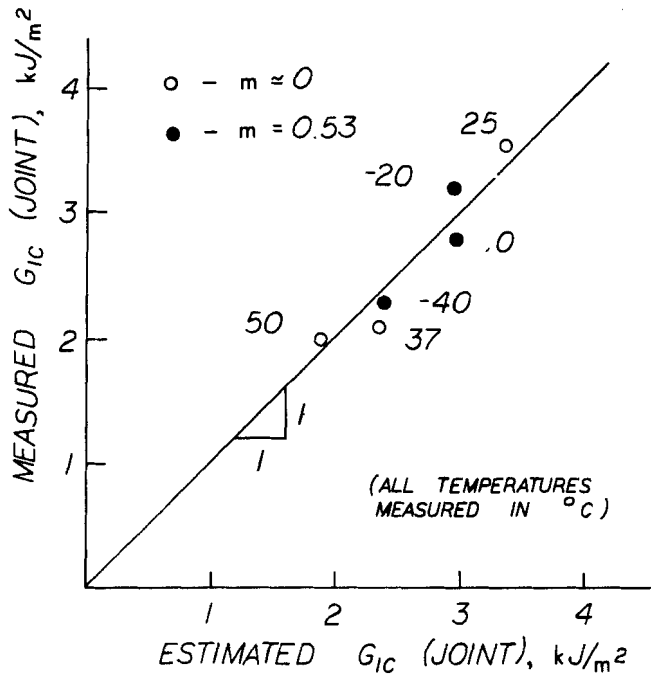


FIGURE 5 Comparison between the measured  $G_{IC}(\text{joint})$  from Bascom and Cottington<sup>2</sup> and the estimated  $G_{IC}(\text{joint})$  from the *in-situ* failure model.

These average values, although at best approximate, do help to demonstrate the controlling material variables at different temperature range. To carry out the correlation, the constants  $m$  and  $M$  in Equation 10 are solved by using the least square method from the material variables from Table I.  $M$  and  $m$  so obtained (Table I) are then used to estimate  $G_{IC}(\text{joint})$  from Equation 8 based on the bulk properties. For the low temperature data,  $m$  is found to be 0.53 which is not much smaller than 1 ( $m = \lambda'$ ) as discussed. The high temperature data, on the other hand, have  $m \approx 0$  which agrees well with  $m = \lambda \ll 1$  anticipated.

A reasonable comparison between the estimated and the measured values of  $G_{IC}(\text{joint})$  is shown in Table I and Figure 5. The straight line in Figure 5 represents the ideal condition of equal estimated and measured values. Although only limited data can be correlated here, the interpretation offered by our model to the results of Bascom and Cottington<sup>2</sup> is quite plausible.

### Test rate effect

$G_{IC}(\text{joint})$  for fixed bond thickness  $h$  may not necessarily follow the same trend of  $G_{IC}(\text{bulk})$  as loading rate changes.  $G_{IC}(\text{bulk})$  usually decreases with increasing test rate. Depending on temperature<sup>3-5</sup> and  $h^{3-5,11}$ ,  $G_{IC}(\text{joint})$  can be an increasing or a decreasing function of loading rate. The observed phenomena, again, are not all that surprising as can be described by our model.

Equation 8 indicates that, depending on the value of  $m$ ,  $(\sigma_y^2/E)$  and  $G_{IC}(\text{bulk})$  may have different weights in determining  $G_{IC}(\text{joint})$ . Unlike  $G_{IC}(\text{bulk})$ ,  $\sigma_y$  and  $E$  both increase with increasing loading rate. The variation of  $\sigma_y$  with loading rate is similar to or even faster than that of  $E^{10}$ . As a result,  $(\sigma_y^2/E)$ , in contrast to  $G_{IC}(\text{bulk})$ , is likely to be an increasing function of loading rate.

As the plastic zone extends to the region with stress of  $r^{-\lambda/2}$  dependence with  $\lambda \ll 1$ ,  $G_{IC}(\text{joint})$ , from Equation 8, will be a stronger function of  $(\sigma_y^2/E)$  than of  $G_{IC}(\text{bulk})$ .  $G_{IC}(\text{joint})$  will thus increase with the loading rate as  $(\sigma_y^2/E)$  does. This at least explains the observations made by Hunston *et al.*<sup>3,5</sup> (for  $h = 0.25$  mm at 23°C and 80°C), Kinloch and Shaw<sup>4</sup> (for  $h = 0.30$  mm) and O'Conner and Brinson.<sup>11</sup>

When the front of plastic zone is in the region of  $r^{-\lambda/2}$  dependent stress with high value of  $\lambda'$ ,  $G_{IC}(\text{joint})$  can be predominantly determined by  $G_{IC}(\text{bulk})$  and thus decreases with increasing loading rate. This happens when  $h$  is large enough so that  $r^{-1/2}$  dependent stress is no longer extremely confined to the crack tip. It may also occur when  $\sigma_y$  is sufficiently high, for example at very low temperature, to limit the growth of plastic zone. Observations that can be described by the argument include the adhesive fracture energies measured by Hunston *et al.*<sup>3,5</sup> (for  $h = 0.25$  mm at -40°C) and Kinloch and Shaw<sup>4</sup> (for  $h = 1.0$  mm).

### Parameters affecting $m$ and $s$

$G_{IC}(\text{joint})$  is a function of a number of test and geometric variables. In our model, the controlling parameters such as  $m$  and  $S$  are affected by the variables summarized below.

The value of  $m$  indicates to what stress region the plastic zone has extended.  $m$  is sensitive to the variables related to yield stress and crack tip stress distribution:  $\sigma_y$ , test rate, temperature, bond thickness  $h$  and

adhesive modulus to adherend modulus ration  $E/E'$ . Some results of stress distribution at different  $h$  and  $E/E'$  can be found in Wang *et al.*<sup>6</sup>

$S$ , a parameter in our approximate failure criterion  $l_p = Sr_p$ , should be a strong function of crack tip stress state.  $S$ , therefore, will be influenced by  $h$  and  $E/E'$ . Other variables have much less effect on stress profile and thus  $S$ .

## CONCLUSION

A theoretical model is proposed to describe the *in-situ* failure process of adhesive joints. The development of a plastic zone at the crack tip is related to the unique stress state induced by a crack in an adhesive joint. As a result, a quantitative representation of  $G_{IC}(\text{joint})$  as a function of adhesive material properties is found. The important finding is that  $G_{IC}(\text{joint})$  is controlled by adhesive yield stress  $\sigma_y$ , Young's modulus  $E$  and bulk resin fracture energy  $G_{IC}(\text{bulk})$ . From our model, the factor  $(\sigma_y^2/E)$  is shown to be sometimes more important than  $G_{IC}(\text{bulk})$  in determining  $G_{IC}(\text{joint})$ . The model interprets well the phenomena of temperature and loading rate dependence of adhesive fracture reported in the literature. The important resin material variables controlling adhesive failure are, therefore, identified.

## References

1. W. D. Bascom, *et al.*, *J. Appl. Polym. Sci.* **19**, 2545 (1975).
2. W. D. Bascom and R. L. Cottingham, *J. Adhesion* **7**, 333 (1976).
3. D. L. Hunston, *et al.*, *J. Elastomers and Plastics* **12**, 133 (1980).
4. A. J. Kinloch and S. J. Shaw, *J. Adhesion* **12**, 59 (1981).
5. J. L. Bitner, *et al.*, *J. Adhesion* **13**, 3 (1981).
6. S. S. Wang, J. F. Mandell and F. J. McGarry, *Intern. J. Fracture* **14**, 39 (1978).
7. S. M. Lee, "Correlation Between Resin Material Variables and Transverse Cracking in Composites", *J. Mater. Sci.* (in press).
8. R. A. Gledhill and A. J. Kinloch, *Polym. Eng. Sci.* **19**, 82 (1979).
9. R. Y. Ting and R. L. Cottingham, *J. Adhesion* **12**, 243 (1981).
10. S. Yamani and R. J. Young, *J. Mater. Sci.* **15**, 1814 (1980).
11. D. G. O'Connor and H. F. Brinson, Virginia Polytechnic Institute and State University, Technical Report VPI-E-79-31, September 1979, PP. 65-68.